

Interacting electron systems between Fermi leads: effective one-body transmissions and correlation clouds

Rafael A. Molina^{1,2}, Dietmar Weinmann³, and Jean-Louis Pichard^{1,4}

¹ CEA/DSM, Service de Physique de l'Etat Condensé, Centre d'Etudes de Saclay, 91191 Gif-sur-Yvette, France

² Max-Planck-Institut für Physik Komplexer Systeme, Nöthnitzer Str. 38, 01187 Dresden, Germany

³ Institut de Physique et Chimie des Matériaux de Strasbourg, UMR 7504 (CNRS-ULP), 23 rue du Loess, BP 43, 67034 Strasbourg Cedex 2, France

⁴ Laboratoire de Physique Théorique et Modélisation, Université de Cergy-Pontoise, 95031 Cergy-Pontoise Cedex, France

Reference: Eur. Phys. J. B **48**, 243-247 (2005)

Abstract. In order to extend the Landauer formulation of quantum transport to correlated fermions, we consider a spinless system in which charge carriers interact, connected to two reservoirs by non-interacting one-dimensional leads. We show that the mapping of the embedded many-body scatterer onto an effective one-body scatterer with interaction-dependent parameters requires to include parts of the attached leads where the interacting region induces power law correlations. Physically, this gives a dependence of the conductance of a mesoscopic scatterer upon the nature of the used leads which is due to electron interactions inside the scatterer. To show this, we consider two identical correlated systems connected by a non-interacting lead of length L_C . We demonstrate that the effective one-body transmission of the ensemble deviates by an amount A/L_C from the behavior obtained assuming an effective one-body description for each element and the combination law of scatterers in series. A is maximum for the interaction strength U around which the Luttinger liquid becomes a Mott insulator in the used model, and vanishes when $U \rightarrow 0$ and $U \rightarrow \infty$. Analogies with the Kondo problem are pointed out.

PACS. 71.27.+a Strongly correlated electron systems; heavy fermions – 72.10.-d Theory of electronic transport; scattering mechanisms – 73.23.-b Electronic transport in mesoscopic systems

1 Introduction

In Landauer's formulation of quantum transport [1], the measure of the conductance g of a coherent system is formulated as a scattering problem between incoherent electron reservoirs. In a two-probe geometry, the system is connected to two reservoirs via leads. For large electron densities, the Coulomb interaction is screened and the Coulomb to kinetic energy ratio r_s is small. One has essentially a non-interacting system of Fermi energy E_F , where the occupation of the one-body levels is given by a Fermi-Dirac distribution at a temperature T . The system acts as a one-body scatterer and its residual conductance $g(T \rightarrow 0)$ is given (in units of $2e^2/h$ for single channel leads and spin degeneracy) by the probability $|t(E_F)|^2$ of an electron of energy E_F to be elastically transmitted through it.

The problem of describing coherent electronic transport becomes more complex in the case where the carrier density is low inside the scatterer, the screening ceasing to be effective and the electrons becoming correlated. Such situations occur in quantum point contacts of transverse size smaller than the Fermi wavelength, where a $0.7 (2e^2/h)$ structure is observed [2], and can be expected

in molecules [3], atomic chains or contacts [4], quantum dots where few electrons might form a correlated solid, a charge density wave, a Mott insulator, etc. In these cases, the electrons are transmitted from one Fermi reservoir to another through a many-body scatterer. To extend Landauer's approach to such systems, at least for low temperatures and bias voltages, one needs to reduce the bare many-body scatterer to an effective one-body scatterer with interaction-dependent parameters. This task will be hopeless for an isolated system where electrons interact with a large interaction strength U , but becomes possible when leads where electrons do not interact are attached to it. This has been numerically demonstrated in previous works [5,6] using the embedding method, which allows to extract [5,6,7,8,9,10,11] the effective coefficient $|t(E_F, U)|^2$ from the persistent current of a large non-interacting ring embedding the many-body scatterer. Using the same method, we show that it is not the region where the electrons interact which acts as an effective one-body scatterer with renormalized parameters, but a larger region where the many-body scatterer induces correlations. This problem is somewhat similar to the Kondo problem, which can be solved using Wilson's numerical renormalization group (NRG) [12]. Instead of using the

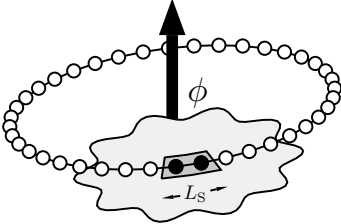


Fig. 1. Scheme of the ring pierced by a flux ϕ used for the embedding method. The correlation cloud induced by L_S interacting sites upon the auxiliary lead is sketched in grey.

NRG method, we use the density matrix renormalization group (DMRG) method [13, 14] for a non-interacting ring embedding the many-body scatterer, as sketched in Fig. 1. The modulus of the effective one-body transmission amplitude $|t(E_F, U)|$ is obtained from the persistent current of the ring extrapolated to infinite lead length, while its phase α is given by the Friedel sum rule.

After a study of the contained extrapolation, we apply the embedding method to determine the effective total transmission coefficient $|t_T(E_F, U)|^2$ of two identical many-body scatterers in series, connected by a non-interacting lead of size L_C (sketched in Fig. 2). The resulting exact value for $|t_T(E_F, U)|^2$ deviates from the one obtained assuming the combination law of one-body scatterers in series. This U -dependent deviation is due to induced correlations in the attached leads, and its dependence on L_C allows to determine the size of the region which acts as an effective one-body scatterer.

2 Embedding method, extrapolation and correlation cloud

To study the mapping of a bare many-body scatterer coupled to leads onto an effective one-body scatterer with interaction-dependent coefficients, we take a model of N spinless fermions in a chain of $L = L_S + L_L$ sites. The Hamiltonian (with even L_L) reads

$$H = -t_h \sum_{i=2}^L (c_i^\dagger c_{i-1} + c_{i-1}^\dagger c_i) + U \sum_{i=L_L/2+2}^{L_L/2+L_S} [n_i - V_+] [n_{i-1} - V_+] . \quad (1)$$

The hopping amplitude $t_h = 1$ between nearest neighbor sites sets the energy scale, c_i (c_i^\dagger) is the annihilation (creation) operator at site i , and $n_i = c_i^\dagger c_i$. The nearest neighbor repulsion U acts upon L_S consecutive sites and gives rise to many-body scattering. We take a half-filled model ($N = L/2$), with a potential $V_+ = 1/2$ being due to a positive background charge which exactly compensates the repulsion U inside the scatterer. Therefore, our model exhibits particle-hole symmetry and a uniform density, without Friedel oscillations around the scattering region where the fermions interact.

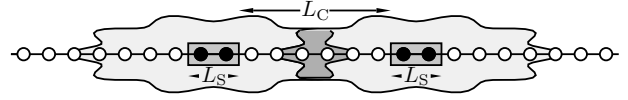


Fig. 2. Scheme of the set-up with two identical many-body scatterers connected by L_C sites where the carriers do not interact. When L_C is small, the two correlation clouds sketched in grey overlap and the effective one-body scatterer of the ensemble is not given by the effective one-body scatterer of each element and the combination law of one-body scatterers in series.

The scattering geometry corresponds to two leads of $L_L/2 \rightarrow \infty$ sites connected by an interacting scatterer of L_S sites. The electrons do not interact in the leads, a necessary condition for having appropriate asymptotic scattering channels in one dimension. For the embedding method, we consider the ring geometry sketched in Fig. 1, the scatterer being closed on itself via a non-interacting lead of L_L sites. This is achieved by adding a hopping term

$$-t_h c_1^\dagger c_L \exp(i\phi) + \text{h.c.}$$

to the Hamiltonian (1), the flux ϕ driving a persistent current $J(U)$ in the ring. As the flux dependence of $J(U)$ extrapolated to the limit $L_L \rightarrow \infty$ demonstrates [6], the many-body scatterer behaves as an effective one-body scatterer, but with an interaction-dependent elastic transmission coefficient $|t(E_F, U)|^2$. Instead of using $J(U)$, it is simpler [6] to get $|t(E_F, U)|^2$ from the charge stiffness

$$D(U, L_S, L) = (-1)^N \frac{L}{2} (E_0(U, L_S, L) - E_\pi(U, L_S, L)) , \quad (2)$$

where $E_0(U, L_S, L) - E_\pi(U, L_S, L)$ is the change of the ground-state energy from periodic to antiperiodic boundary conditions. $D(U, L_S, L)$ is obtained by the DMRG implementation for real Hamiltonians, which can be used to study with a great accuracy systems as large as $L = 120$ sites with $N = 60$ particles. In the limit $L_L \rightarrow \infty$, one gets the modulus

$$|t(E_F, U)| = \sin \left(\frac{\pi}{2} \frac{D_\infty(U, L_S)}{D_\infty(U=0, L_S)} \right) \quad (3)$$

of the transmission amplitude through the scatterer of L_S sites, $D_\infty(U=0, L_S)$ being the charge stiffness of the same ring for $U=0$.

To take the limit $L_L \rightarrow \infty$ is one of the key points of the embedding method. This extrapolation is also required for pure one-body scattering, where the finite size corrections to formula (3) can be expanded [6] in powers of $1/L$. For many-body scattering, the DMRG study gives an empirical scaling law [5, 6]

$$D(U, L_S, L) = D_\infty(U, L_S) \exp \left(\frac{C(U, L_S)}{L} \right) \quad (4)$$

obtained for large L_L and small L_S , which allows to determine the asymptotic value $D_\infty(U, L_S)$ necessary to obtain

$|t(E_F, U)|^2$. Expanding this scaling law gives

$$D(U, L_S, L) - D_\infty(U, L_S) \approx \frac{B(U, L_S)}{L} \quad (5)$$

when L is large enough, where

$$B(U, L_S) = C(U, L_S)D_\infty(U, L_S). \quad (6)$$

This is a power law decay, and not an exponential decay with a characteristic scale above which the finite size correction can be neglected. Numerical data show that $B(U, L_S)$ is important for intermediate interaction strengths U . But in the limits $U \rightarrow 0$ (no scattering, total transmission) and $U \rightarrow \infty$ (total reflection, $D_\infty(U \rightarrow \infty, L_S) \rightarrow 0$), the finite size corrections vanish and $B(U, L_S) \rightarrow 0$.

However, since adding one-body potentials in the region of the L_S sites yields a finite size correction to $D(U, L_S, L)$ even when $U \rightarrow 0$, the interpretation of these corrections is not straightforward. They do not depend only on the correlations induced in the attached lead by the interaction acting inside the scatterer, but also on more trivial one-body aspects.

3 Combination of two many-body scatterers in series

A more direct approach, where the finite size effects are only due to many-body correlations, consists in taking two identical scatterers connected by a scattering-free lead of size L_C in which the electrons do not interact, as sketched in Fig. 2. Since the scattering channels begin at the first attached sites of the leads when $U = 0$, there is a simple combination law for one-body scatterers in series. To study how this combination law is broken with increasing U when L_C is small allows to show that the size of the effective elastic scatterer is larger than the region where the carriers interact. When $U \neq 0$, the scattering channels begin only asymptotically far from the many-body scatterer.

Without interaction, a scatterer can be described at energy E_F by a unitary scattering matrix S_S , written in terms of its reflection and transmission amplitudes r, r' and t, t' as

$$S_S = \begin{pmatrix} r & t' \\ t & r' \end{pmatrix}. \quad (7)$$

The scatterer being symmetric upon time reversal, one has $t = t'$, while $r = r'$ if the scatterer is symmetric upon space inversion. The transfer matrix M_S (giving the flux amplitudes at the right side in terms of the flux amplitudes at the left side) reads

$$M_S = \begin{pmatrix} 1/t & r/t \\ r^*/t^* & 1/t^* \end{pmatrix}. \quad (8)$$

The total Hamiltonian and the parity operator can be simultaneously diagonalized if one has inversion symmetry, to give even and odd standing-wave solutions which can

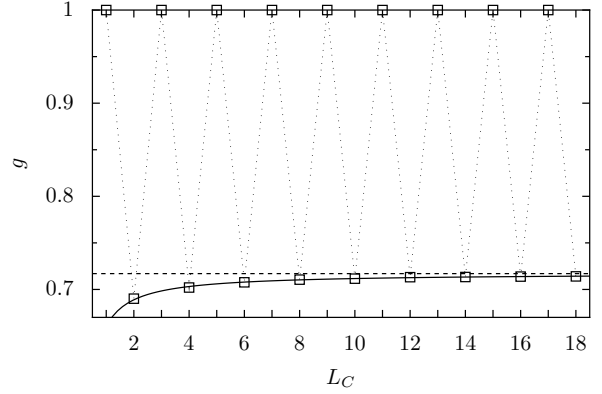


Fig. 3. Conductance $g(L_C)$ of the set-up sketched in Fig. 2 with $L_S = 2$, for $U = 1$. The points are obtained with the embedding method for the ensemble. The dashed line at $g = 0.717$ gives the approximate value obtained from Eq. (15), with $|t|$ obtained by the embedding method for a single scatterer. The solid line is a fit with the form $g(L_C) = 0.7174 - 0.057/L_C$.

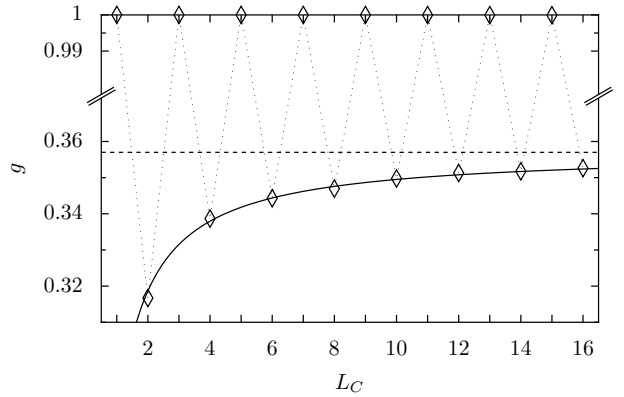


Fig. 4. Conductance $g(L_C)$ as in Fig. 3, but for $U = 2$. The dashed line at $g = 0.357$ represents the value yielded by Eq. (15), and the solid line is the fit $g(L_C) = 0.3572 - 0.077/L_C$.

be written as $\psi_i^0 = \cos(ki + \delta_0)$ and $\psi_i^1 = \sin(ki + \delta_1)$ at the right side of the scatterer, and $\psi_i^0 = \cos(ki - \delta_0)$ and $\psi_i^1 = \sin(ki - \delta_1)$ at its left side. The two phase shifts δ_0 and δ_1 are related [15] to t and r by

$$\begin{aligned} t &= (\exp(2i\delta_0) + \exp(2i\delta_1))/2, \\ r &= (\exp(2i\delta_0) - \exp(2i\delta_1))/2. \end{aligned} \quad (9)$$

Due to symmetries, S_S or M_S have only two free parameters: the modulus $|t| = \cos(\delta_0 - \delta_1)$ and the phase $\alpha = \delta_0 + \delta_1$ of the transmission amplitude t , the unitarity of S_S ($|t|^2 + |r|^2 = 1$ and $r/r^* = -t/t^*$) giving r . We can determine $|t|$ by the embedding method. The Friedel sum rule [16] gives α . If one introduces a scatterer with inversion symmetry in the central region of a scattering free lead, this rule states [17] that

$$\alpha = \delta_0 + \delta_1 = \pi N_f \quad (10)$$

for spinless fermions in one dimension. N_f is the number of displaced fermions when the scatterer is introduced in

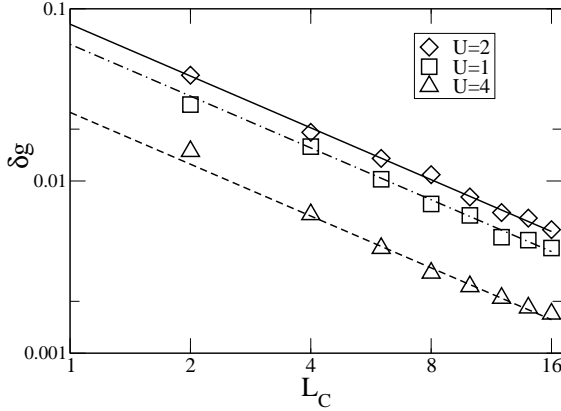


Fig. 5. Error δg made when using the combination law of Eq. (14) for having the conductance of the set-up sketched in Fig. 2 with $L_S = 2$ and different values of U , as a function of an even number L_C of connecting sites. The lines give an $A(U, L_S)/L_C$ fit.

the central region. For a uniform filling factor $\nu = 1/2$, $N_f = L_S/2$, and the phase α reads

$$\alpha = \pi N_f = \frac{\pi L_S}{2} = k_F L_S, \quad (11)$$

where $k_F = \pi/2$ is the Fermi wave number. For the spinless case in one dimension with a uniform density, this simply means that the transmitted wave has N_f changes of sign when one transfers a fermion through a scatterer containing N_f others. This is obvious for $U = 0$ as well as for $U \neq 0$. Using the same rule, the ideal ballistic lead of L_C sites has a modulus $|t(L_C)| = 1$ and a phase $\alpha(L_C) = k_F L_C$. Its transfer matrix reads

$$M_C = \begin{pmatrix} e^{-ik_F L_C} & 0 \\ 0 & e^{ik_F L_C} \end{pmatrix}. \quad (12)$$

The combination law of one-body scatterers in series being a simple matrix multiplication for the transfer matrices, the total transfer matrix $M_T(E_F)$ of the ensemble is given by

$$M_T = M_S \cdot M_C \cdot M_S. \quad (13)$$

For the total transmission coefficient $|t_T|^2$ through the ensemble, expressed in terms of the transmission t of each element and of L_C , this gives

$$|t_T|^2 = \frac{|t|^4}{2(1 - |t|^2)(1 + \cos(2k_F L_C - 2\alpha)) + |t|^4}. \quad (14)$$

Since $|t| = 1$ when L_S is odd [5,18], we consider only even values of L_S . Taking $\alpha = \pi L_S/2$ gives the Landauer conductance $g = |t_T|^2 = 1$ if L_C is odd and

$$g = \frac{|t|^4}{(|t|^2 - 2)^2} \quad (15)$$

for L_C even.

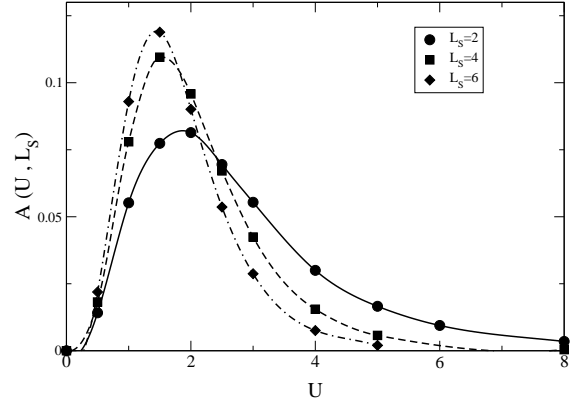


Fig. 6. Amplitude $A(U, L_S)$ of the fits shown in Fig. 5 as a function of U for different values of L_S .

4 Correlation-induced deviations from the non-interacting combination law

Fig. 3 and 4 show the conductance g for two scatterers of $L_S = 2$ sites in series, as a function of the length L_C of the coupling lead. The data points are directly obtained from the embedding method, without assuming a combination law for scatterers in series. Resonances with $g = 1$ occur for odd $L_C = \{1, 3, 5, \dots\}$. For even L_C , the dashed lines represent the L_C -independent values $|t|^4/(|t|^2 - 2)^2$ implied by Eq. (14), the coefficient $|t|$ being obtained using the embedding method for a single scatterer. Within the accuracy of the extrapolation procedures required for having the transmission $|t|$ of an individual scatterer and the total conductance g , the result of (14) gives the correct value when $L_C \rightarrow \infty$, but overestimates g for small even values of L_C . The difference

$$\delta g(L_C) = g(L_C \rightarrow \infty) - g(L_C) \quad (16)$$

is shown in Fig. 5 for even L_C at different values of U . For even L_C , $\delta g(L_C)$ decays as a function of L_C as

$$\delta g(L_C) \approx \frac{A(U, L_S)}{L_C}, \quad (17)$$

with an amplitude $A(U, L_S)$ which is shown in Fig. 6 as a function of the interaction strength U . This $1/L_C$ decay is reminiscent of the $1/L$ decay characterizing $D(U, L_S, L) - D_\infty(U, L_S)$ and of the screening at large distances (larger than the Thomas-Fermi screening length) of the potential of a point charge by non-interacting electrons (Friedel oscillations, RKKY interactions ...) in one dimension. This suggests that the decay could be faster for leads of higher dimensions ($1/L_C^d$ decay in d dimensions). The amplitude $A(U, L_S) \rightarrow 0$ when $U \rightarrow 0$ (one-body scatterers) and when $U \rightarrow \infty$. In this latter limit, the scatterers become decoupled from the leads, the energy for an electron to enter or to leave a scatterer being $\propto U$. $A(U)$ is maximum near $U = 2$, a value where in the thermodynamic limit $L_S \rightarrow \infty$ the Luttinger liquid becomes [19] a Mott insulator for spinless fermions.

For all odd values of L_C , the data for the total transmission coincide with the value $g = 1$ obtained from Eq. (14), and $\delta g(L_C) = 0$. The even-odd dependence on the parity of L_C shows that the convergences of the phase α and the modulus $|t|$ of the effective scatterer are characterized by different scales. One has $\alpha = \pi N_f$ across the scatterer, directly on a scale L_S , independently of U , while $|t|$ reaches its asymptotic value on a much larger scale. This is not surprising since α depends on the mean density, while $|t|$ depends on the correlations of its fluctuations. In our model with a compensating background charge, the mean density does not exhibit Friedel oscillations. Let us underline that the correlation clouds which have to be included with the many-body scatterer to form the effective one-body scatterer must not be confused with the screening clouds characterizing the charge density.

5 Discussion of the relation to the Kondo problem

To obtain the effective one-body matrix $S(E_F)$ of a correlated system of spinless fermions is a problem which displays a certain similarity with the Kondo problem of a spin degree of freedom surrounded by a metallic host. In the two cases, it is crucial to couple the many-body system to non-interacting conduction electrons. For the Kondo problem, the original $3d$ model can be mapped onto a $1d$ lattice without interaction embedding a Hubbard impurity. In Wilson's renormalization group transformations [12], the embedded many-body Hamiltonian is progressively mapped onto an effective one-body Hamiltonian describing the low energy states. In this transformation, the coupling between different length scales is taken into account progressively, working out from the impurity to the longer length scales and lower energies. The states at sites near the impurity involve conduction states spanning the full band width $2t_h$, while the states located far from the impurity involve conduction states near the Fermi level, with a progressively reduced band width. This NRG method has been used recently [20] to calculate the effective one-body Hamiltonian of a few Hubbard sites embedded in a non-interacting chain, and the corresponding phase shifts.

In our spinless case, the embedded system would give rise to inelastic and elastic scattering if it was in the vacuum. Due to the attached non-interacting leads inelastic processes become progressively blocked by a Fermi vacuum which eventually takes place in the leads, at a large distance from the scatterer. Our DMRG study leads us to a similar conclusion as NRG studies of impurities with spin. It shows that the effective one-body elastic scatterer necessary for extending the Landauer formulation of coherent transport to correlated fermion systems must include parts of the attached leads where the interacting region induces power law correlations. Physically, this gives a dependence of the conductance of a mesoscopic scatterer upon the nature of the used leads which depends on the strength of the interactions inside the scatterer. Eventually, let us mention that the vertex corrections due to

inelastic scattering vanish [21] when $T \rightarrow 0$, in a perturbative approach to the Kubo conductance of an interacting region embedded between semi-infinite leads. While this agrees with our findings for $L_L \rightarrow \infty$, it is likely that these corrections do not vanish when L_L is finite, and exhibit similar power-law decays as L_L increases.

6 Acknowledgments

We thank Y. Asada, G.-L. Ingold, R.A. Jalabert, O. Sushkov and G. Vasseur for stimulating discussions, and P. Schmitteckert for his DMRG code. R.A. Molina acknowledges the financial support provided through the European Community's Human Potential Program under contract HPRN-CT-2000-00144.

References

1. R. Landauer, IBM J. Res. Dev. **1**, 223 (1957); M. Büttiker, Phys. Rev. Lett. **57**, 1761 (1986); Y. Imry, *Introduction to Mesoscopic Physics*, Oxford University Press (1997).
2. K.J. Thomas, J.T. Nicholls, M.Y. Simmons, M. Pepper, D.R. Mace, and D.A. Ritchie, Phys. Rev. Lett. **77**, 135 (1996).
3. C. Kergueris, J.-P. Bourgoin, S. Palacin, D. Esteve, C. Urbina, M. Magoga, and C. Joachim, Phys. Rev. B **59**, 12505 (1999).
4. N. Agrait, A.L. Yeyati, and J.M. van Ruitenbeek, Phys. Rep. **377**, 81 (2003).
5. R.A. Molina, D. Weinmann, R.A. Jalabert, G.-L. Ingold, and J.-L. Pichard, Phys. Rev. B **67**, 235306 (2003).
6. R.A. Molina, P. Schmitteckert, D. Weinmann, R.A. Jalabert, G.-L. Ingold, and J.-L. Pichard, Eur. Phys. J. B **39**, 107 (2004).
7. A.O. Gogolin and N.V. Prokof'ev, Phys. Rev. B **50**, 4921 (1994).
8. J. Favand and F. Mila, Eur. Phys. J. B **2**, 293 (1998).
9. O.P. Sushkov, Phys. Rev. B **64**, 155319 (2001).
10. V. Meden and U. Schollwöck, Phys. Rev. B **67**, 193303 (2003).
11. T. Rejec and A. Ramšak, Phys. Rev. B **68**, 035342 (2003).
12. A.C. Hewson, *The Kondo Problem to Heavy Fermions*, Cambridge University Press (1993).
13. S.R. White, Phys. Rev. Lett. **69**, 2863 (1992); Phys. Rev. B **48**, 10345 (1993).
14. *Density Matrix Renormalization – A New Numerical Method in Physics*, ed. by I. Peschel, X. Wang, M. Kaulke and K. Hallberg, Lecture Notes in Physics, Vol. 528, Springer, Berlin (1999).
15. H.J. Lipkin, *Quantum Mechanics, New Approaches to Selected Topics*, North Holland (1973).
16. J. Friedel, Phil. Mag. **43**, 153 (1952).
17. J.S. Langer and V. Ambegaokar, Phys. Rev. **121**, 1090 (1961); D.C. Langreth, Phys. Rev. **150**, 516 (1966).
18. R.A. Molina, D. Weinmann, and J.-L. Pichard, Europhys. Lett. **67**, 96 (2004).
19. T. Giamarchi, *Quantum Physics in One Dimension*, Oxford University Press (2004).
20. A. Oguri, Y. Nisikawa, and A.C. Hewson, J. Phys. Soc. Jpn. **74**, 2553 (2005) and references therein.
21. A. Oguri, J. Phys. Soc. Jpn. **66**, 1427 (1997).